

Joint Estimation of Time of Arrival and Channel Power Delay Profile for Pulse-Based UWB Systems

Fang Shang, Benoit Champagne and Ioannis Psaromiligkos
 Department of Electrical and Computer Engineering, McGill University
 3480 University Street, Montreal, Quebec, Canada, H3A 2A7

Email: fang.shang@mail.mcgill.ca; benoit.champagne@mcgill.ca; ioannis.psaromiligkos@mcgill.ca

Abstract—Sub-Nyquist maximum likelihood (ML)-based time of arrival (TOA) estimation methods for ultra-wideband (UWB) signals normally assume *a priori* knowledge of the UWB channel in the form of the average power delay profile (APDP). In practice however, and despite its importance, the APDP is not always available. To address this issue, we develop in this paper a joint estimator of TOA and APDP. Knowing that the APDP of a UWB channel usually consists of several clusters, each with specific exponential decay rate, a parametric APDP model of this type is employed. The parameters of this model are estimated via a least-squares fitting approach; then the estimated APDP is used to form a likelihood function and obtain a ML estimator of the TOA. Simulations show that the TOA estimated jointly in this way achieves a good accuracy in practical scenarios. The proposed APDP estimate can also help to boost the performance of previously reported TOA estimators that assume *a priori* APDP knowledge, although the proposed ML scheme generally offers superior performance.

Index Terms—ultra wideband (UWB), time of arrival (TOA) estimation, average power delay profile (APDP), maximum likelihood (ML)

I. INTRODUCTION

In recent years, ultra-wideband (UWB) communications and localization systems have drawn extensive attention. In UWB impulse-radio (IR) systems, pulses with very short duration are transmitted over the air. The resulting very wide bandwidth of UWB signals ensures that they can provide very accurate temporal measurements, which can be used for precise time of arrival (TOA) estimation.

There exist many TOA estimators for UWB systems. Early works [1], [2] focus on TOA estimation based on the maximum likelihood (ML) approach with explicit consideration of the multipath propagation structure. In particular, it is shown that the performance of these ML estimators approaches the Cramer-Rao bound (CRB) at high signal-to-noise ratios (SNRs). Though they can achieve good TOA estimation accuracy, their requirement of Nyquist rate sampling of the received signals and the computational complexity of estimating a large number of multipaths make them impractical due to the high implementation costs. Therefore, recent works have focused on lower sampling rate and low-complexity TOA estimation algorithms.

Energy detection (ED) receivers [3], [4], [5] have become quite popular due to their low complexity. Within this class,

[3] proposed a two-step approach, in which TOA estimation is performed by first obtaining a coarse TOA estimate based on ED, and then refining the estimate via hypothesis testing. The performance of low-sampling rate matched filter (MF) and ED for TOA estimation based on thresholding is analyzed and compared in [4]. Two new Bayesian TOA estimators that rely on the overall energy profile available at the output of the ED are proposed in [5]. A main disadvantage of ED receivers is that they may suffer greatly from noise and their performance thus degrades rapidly at lower SNR.

ML estimators based on sub-Nyquist sampling models have also been proposed, such as ML estimator with partial channel information (MLP) [6], weighted maximum energy sum selection (W-MESS) and double-weighted maximum energy sum selection (DW-MESS) [7]. In [8], ML timing estimation with sub-sampling is proposed under the assumptions of normally distributed channels and knowledge of the average power delay profile (APDP). These sub-Nyquist sampling and low complexity ML estimators can achieve good estimation accuracy, but to function properly, they generally require *a priori* information about the channel, in the form of the APDP, which should be estimated beforehand.

In this work, we propose to jointly estimate the APDP along with the TOA, since the knowledge of the APDP may not be available in practice. According to the IEEE 802.15.4a standard [9], we assume a simplified multiple cluster parametric model, each cluster being characterized with its own energy level, exponential decay rate and time offset. The parameters of this model are estimated via a least-squares (LS) fitting approach; then the estimated APDP is used to form a likelihood function and obtain a ML estimator of the TOA. Simulations show that the TOA estimated jointly in this way can achieve sub-nanosecond accuracy in practical scenarios. The proposed APDP estimate can also help boost the performance of previously reported sub-Nyquist TOA estimators which need APDP beforehand, although the proposed ML scheme generally offers superior performance.

The rest of this paper is organized as follows. Section 2 gives a description of the system model. Section 3 presents the derivation of the underlying log likelihood function. Section 4 presents the proposed joint TOA and APDP estimation approach. Simulation results are discussed in Section 5 and the last section concludes the paper.

This work was supported in part by the Fonds Québécois de la Recherche sur la Nature et les Technologies.

II. SIGNAL AND SYSTEM MODEL

TOA estimation is normally performed during a preamble section of a packet, where no data is transmitted. We consider a time hopping (TH) IR-UWB system. In the observation interval T_o , there are N_f consecutive frames of duration T_f , i.e., $T_o = N_f T_f$. In turn, each frame is divided into N_c consecutive chips of equal duration T_c , so that $T_f = N_c T_c$. Within the j th frame, $j \in \{0, 1, \dots, N_f - 1\}$, a single IR-UWB pulse $w(t)$ of duration T_c is transmitted with a time offset of $c_j T_c$ relative to the beginning of the frame, where $c_j \in \{0, \dots, N_c - 1\}$ denotes the TH sequence. In addition, the pulse transmitted within the j th frame is affected by a polarity code, $d_j \in \{+1, -1\}$, used for spectrum smoothing [10]. Therefore, the transmitted signal $s(t)$ is given by

$$s(t) = \sum_{j=0}^{N_f-1} d_j \sqrt{E_p} w(t - jT_f - c_j T_c), \quad 0 \leq t \leq T_o \quad (1)$$

where $w(t)$ is assumed to have unit energy and E_p denotes the transmitted energy per pulse. In practice, both sequences c_j and d_j are known to the receiver. In this work, since we consider the single user case, no TH code will be used; without loss in generality, we therefore set $c_j = 0, \forall j$.

The UWB signal $s(t)$ propagates over a multipath channel before reaching the tag reader. A tapped delay line model is used here to represent this channel, as in [3], [11]. Assuming a tap spacing of T_c , this model represents the impulse response $h(t)$ of the channel as the sum of scaled and delayed impulses:

$$h(t) = \sum_{l=0}^{L-1} a_l \delta(t - \tau_l) \quad (2)$$

where $\delta(\cdot)$ is the Dirac delta function, a_l is a zero-mean random variable representing the amplitude of the l th multipath component, $\tau_l = lT_c + \tau_0$ is the propagation time delay of the l -th multipath, $\tau_0 > 0$ is the deterministic but unknown delay of the first path, and L is the number of time resolvable multipaths. According to (2), the channel delay spread is given by $\tau_{ds} = LT_c$. In this work, the focus is on sub-Nyquist TOA resolution (chip level uncertainty) and hence we consider the case where τ_0 is an integer multiple of the sub-Nyquist sampling period, i.e., $\tau_0 = DT_c$. Since the above tapped delay line model is based on the use of resolvable time delay bins, the temporal correlation coefficients between adjacent tap amplitudes are very small and can be neglected according to previous studies [8], [12]. Therefore, the channel tap vector, defined as $\mathbf{h} = [a_0, \dots, a_{L-1}]^T$, has a zero mean and a diagonal covariance matrix \mathbf{R}_h . The diagonal entries of \mathbf{R}_h , $P_l = E[a_l^2]$, $l = 0, \dots, L-1$, constitute the APDP of the channel, i.e., $\mathbf{P} = [P_0, \dots, P_{L-1}]^T$.

After multipath propagation, the received UWB signal at the tag reader can be expressed as

$$r(t) = \sum_{l=0}^{L-1} a_l s(t - \tau_l) + n(t), \quad 0 \leq t \leq T_o \quad (3)$$

where $n(t)$ is an additive noise term modeled as a white Gaussian process with zero mean and power spectral density level σ_n^2 . We assume that T_f is sufficiently large such that there is no inter-frame interference.

In order to derive the ML-based joint estimator, an equivalent discrete-time version of the above signal model will be used. We consider uniform sampling at the Nyquist-rate $1/T_s$, where $T_s = 1/2B$ and B is the bandwidth of the transmitted IR signal. Let $M = T_c/T_s$ be an integer, so that each frame is represented by MN_c samples and let $\mathbf{r}_j = [r(jT_f), \dots, r(jT_f + (MN_c - 1)T_s)]^T$ denote the column vector of discrete-time noisy signal samples of the j th frame. Similarly, the IR pulse $w(t)$ of duration T_c can be represented by the column vector $\mathbf{w} = [w(0), \dots, w((M-1)T_s)]^T$. We emphasize that the Nyquist-sampling mentioned here is used only to analyze the discrete-time system model; in the end, the proposed estimator will only require the evaluation of the ML function at the sub-Nyquist chip rate $1/T_c$.

Making use of (3), the vector of received signal samples \mathbf{r}_j in the j th frame can be written as

$$\mathbf{r}_j = d_j \sqrt{E_p} \mathbf{W} \mathbf{h} + \mathbf{n}_j \quad (4)$$

where $\mathbf{W} = [\mathbf{w}_D, \mathbf{w}_{D+1}, \dots, \mathbf{w}_{D+L-1}]$ is a $MN_c \times L$ matrix with columns

$$\mathbf{w}_d = \underbrace{[0, \dots, 0]_{dM}}_{dM}, \mathbf{w}^T, \underbrace{[0, \dots, 0]_{MN_c - M - dM}}_{MN_c - M - dM} \quad (5)$$

for $d \in \{D, D+1, \dots, D+L-1\}$, and \mathbf{n}_j is the discrete-time representation vector of the noise $n(t)$ in the j th frame.

III. ML ESTIMATOR FORMULATION

Given the set of observations \mathbf{r}_j , for $j \in \{0, \dots, N_f - 1\}$, our aim is to develop practical estimators for the unknown integer delay, D , and the APDP vector \mathbf{P} . In this section, we begin by deriving the underlying likelihood function for the joint ML estimation of these parameters. In the next section, we will further exploit available knowledge about the APDP of practical UWB channels, in the form of a low-dimensional parametric model, to simplify the joint estimation.

We model \mathbf{h} as a Gaussian random vector with zero mean and covariance matrix \mathbf{R}_h , independent of the additive noise vector \mathbf{n}_j . It immediately follows from (4) that the vector \mathbf{r}_j is also Gaussian with zero mean and covariance matrix

$$\mathbf{R}_{\mathbf{r}_j} = E[\mathbf{r}_j \mathbf{r}_j^T] = E_p \mathbf{W} \mathbf{R}_h \mathbf{W}^T + \sigma_n^2 \mathbf{I}. \quad (6)$$

In addition, the covariance matrix between observation vectors in different frames is simply

$$\mathbf{R}_{\mathbf{r}_i \mathbf{r}_j} = E[\mathbf{r}_i \mathbf{r}_j^T] = d_i d_j E_p \mathbf{W} \mathbf{R}_h \mathbf{W}^T. \quad (7)$$

Therefore, the covariance matrix of the complete received signal vector within the observation time $T_o = N_f T_f$, represented by $\mathbf{r} = [\mathbf{r}_1^T, \dots, \mathbf{r}_{N_f}^T]^T$, is given by the following block matrix

$$\mathbf{R}_{\mathbf{r}} = E_p \mathbf{W}_r \mathbf{R}_h \mathbf{W}_r^T + \sigma_n^2 \mathbf{I} \quad (8)$$

where $\mathbf{W}_r = \mathbf{d} \otimes \mathbf{W}$, $\mathbf{d} = [d_0, \dots, d_{N_f-1}]^T \in \mathbf{C}^{N_f}$ and \otimes represents the Kronecker product.

Under the Gaussian assumption, the log-likelihood function of the received signal \mathbf{r} can be written in following form:

$$L(\mathbf{r}, \boldsymbol{\theta}) = -\mathbf{r}^T \mathbf{R}_r^{-1} \mathbf{r} - \ln(\det(\mathbf{R}_r)) \quad (9)$$

where $\boldsymbol{\theta} = (P_0, \dots, P_{L-1}, D)$ is the vector of unknown parameters. Here, although not indicated explicitly to simplify the presentation, this dependence is through the covariance matrix $\mathbf{R}_r \equiv \mathbf{R}_r(\boldsymbol{\theta})$ in (9).

After some manipulations and omitting the constant term, (9) becomes

$$L(\mathbf{r}, \boldsymbol{\theta}) = \frac{E_p}{\sigma_n^4} \mathbf{z}^T (\mathbf{R}_h^{-1} + \frac{E_p}{\sigma_n^2} N_f \mathbf{I})^{-1} \mathbf{z} - \ln \det(\frac{E_p}{\sigma_n^2} N_f \mathbf{R}_h + \mathbf{I}) \quad (10)$$

where $\mathbf{z} = \mathbf{W}_r^T \mathbf{r}$ is the matched filter output vector sampled at rate T_c and shifted by D . That is, the l -th entry of \mathbf{z} is given by

$$z(l) = \sum_{j=0}^{N_f-1} d_j \mathbf{w}_{D+l}^T \mathbf{r}_j \quad l = 0, \dots, L-1. \quad (11)$$

After further simplification, the log likelihood function becomes

$$L(\mathbf{r}, \boldsymbol{\theta}) = \sum_{l=0}^{L-1} \left\{ \frac{E_p}{\sigma_n^4} \frac{z(l)^2}{\frac{1}{P_l} + \frac{N_f E_p}{\sigma_n^2}} - \ln \left(1 + \frac{N_f E_p}{\sigma_n^2} P_l \right) \right\} \quad (12)$$

where, we recall, $z(l)$ is a function of D .

The joint ML estimator of delay D and ADPD vector \mathbf{P} can be obtained by maximizing the log-likelihood function with respect to these parameters. Unfortunately, due to the large dimension (i.e., $L+1$) of the resulting parameter vector $\boldsymbol{\theta}$, a practical implementation of this search remains prohibitive. In the next section, we develop a simplified scheme based on a lower-dimensional parametric model of the APDP.

IV. PROPOSED JOINT ESTIMATOR OF TOA AND APDP

If the APDP \mathbf{P} were known, we could estimate the TOA from (12) via a simple one-dimensional (discrete) search. Motivated by this observation, we propose to first estimate the APDP. To this end, we first introduce a parametric model for the ADPD, and then present a simplified algorithm for estimating the model parameters based on LS fitting.

According to the IEEE 802.15.4a task group [9], the APDP conforms to the double-exponential decay model with Poisson inter-arrival time. In this work, we use a simplified and discretized version of that model which expresses the APDP as a sum of multiple, exponentially decaying clusters, as follows:

$$P_l = \sum_{k=0}^{C-1} \beta_k e^{-\alpha_k(l-C_k)} u(l-C_k), \quad l = 0, \dots, L-1 \quad (13)$$

where C is the total number of clusters, $k \in \{0, \dots, C-1\}$ is the cluster index, the non-negative parameters β_k , α_k and $C_k \geq 0$ represent the peak power level, exponential decay rate and starting time of the k th cluster, respectively, and $u(l)$

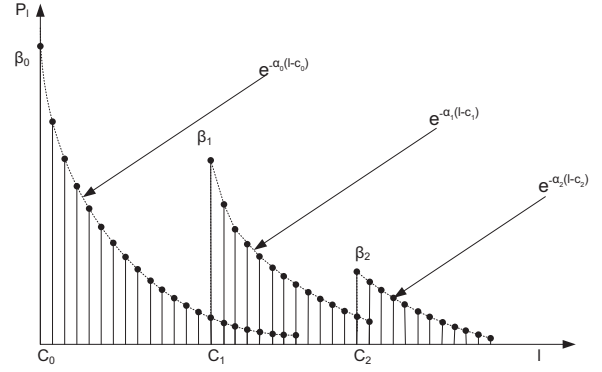


Fig. 1. APDP in simplified Saleh-Valenzuela model.

denotes the unit step function (i.e., $u(l) = 1$ for $l \geq 0$ and 0 otherwise). The corresponding APDP model is illustrated in Fig 1.

Differentiating (9) with respect to \mathbf{R}_h and setting the derivative to zero, the APDP that maximizes the likelihood function assuming a fixed D can be shown to satisfy

$$\hat{P}_l^{(0)} = \frac{1}{E_p} (\bar{z}(l)^2 - \sigma_n^2), \quad l = 0, \dots, L-1, \quad (14)$$

where $\bar{z}(l) = z(l)/N_f$ is the averaged and shifted correlator output.

Intuitively, we would like to adjust the parameters in the model equation (13) so as to achieve the best fit with the available APDP estimate $\hat{\mathbf{P}}^{(0)} = [\hat{P}_0^{(0)}, \dots, \hat{P}_{L-1}^{(0)}]$. Since the clusters decay exponentially on a linear scale, they will be displayed as straight lines with constant slopes after applying a log operation. Therefore, we propose to do the curve fitting in the log domain, i.e.,

$$\min_{C_k, C, \alpha_k, \beta_k} \sum_{l=0}^{L-1} |\ln \hat{P}_l^{(0)} - \ln P_l|^2. \quad (15)$$

In practice, when D is unknown, we obtain the power data \hat{P}_i of the entire frame given by

$$\hat{P}_i = \frac{1}{E_p} (\bar{Z}(i)^2 - \sigma_n^2), \quad i = 0, \dots, N_c - 1. \quad (16)$$

where $\bar{Z}(i)$ is the averaged correlator output given by

$$\bar{Z}(i) = \frac{1}{N_f} \sum_{j=0}^{N_f-1} d_j \mathbf{w}_i^T \mathbf{r}_j \quad i = 0, \dots, N_c - 1. \quad (17)$$

Note that to ensure that $\hat{P}_i > 0$, we can simply adopt the absolute value of the right hand side of (16).

Before we perform the LS fitting in (15), we have to select a rough estimate of D and the corresponding fitting data $\hat{\mathbf{P}}^{(0)}$.

To obtain the preliminary estimate of D , say \hat{D}_r , we use a method similar with the maximum energy sum selection (WESS) [7] method, with the main difference that a threshold is adopted to rule out impossible timing points, which can greatly reduce the computation cost. Once the fitting range is

fixed, we will iteratively search for clusters and do LS fitting for each one.

A detailed description of the algorithm is as follows.

Step 1: We fit the local maxima ($\ln \hat{P}_i > \ln \hat{P}_{i-1}$ and $\ln \hat{P}_i > \ln \hat{P}_{i+1}$) of the whole frame log power data (i.e., $\ln \hat{P}_i, i = 0, \dots, N_c - 1$) to a straight line $l_{TH_1}(i) = \ln \beta - i\alpha$, and set this straight line as a basic threshold. Let α, β be the parameters of the fitted straight line, obtained by minimizing

$$\arg \min_{\alpha, \beta} \sum_{i=0}^{N_c-1} \mu_i |\ln \hat{P}_i - (\ln \beta - i\alpha)|^2. \quad (18)$$

where $\mu_i = 1$ if \hat{P}_i is a local maximum and 0 otherwise. The use of l_{TH_1} will greatly reduce the search range for the rough estimate of \hat{D}_r in the next step.

Step 2: We identify the local maxima of $\ln \hat{P}_i$ which are above the basic threshold $l_{TH_1}(i)$. Among these local maxima, we consider those in the range $0 \leq i \leq D_{max}$ (D_{max} is the largest possible delay). For each of these points, considering its delay as a temporary D , we calculate the corresponding sum $\sum_{l=0}^{L-1} \ln \hat{P}^{(0)}(l)$. The value of the temporary D for which this sum is maximum is taken as the rough estimate \hat{D}_r . The latter also gives us the position of the first cluster in the frame, i.e., $C_0 = \hat{D}_r$ and thus we obtain the fitting data $\hat{P}^{(0)}$.

Step 3: We fit the local maxima of $\hat{P}^{(0)}$ to a new straight line denoted by $l_{TH_2}(l)$, using a similar procedure with step 1. This new threshold, obtained using the data of all the clusters, will be used to determine the onset of any new cluster, that is: the ADPD value at the starting point of each cluster, given by parameter β_k , should be above $l_{TH_2}(l)$.

Step 4: We search for new clusters using $l_{TH_2}(l)$ as a new threshold. Assuming that the starting time of the current cluster C_k is known, we detect a new cluster if we can find at least one point $\hat{P}_l^{(0)}$ that is above $l_{TH_2}(l)$ in the range $C_k + \lceil \tau_{ic}/T_c \rceil \leq i \leq C_k + L$, where τ_{ic} is the minimum inter-cluster delay depending on the channel environment, e.g., $\tau_{ic} = 10\text{ns}$. We denote the corresponding abscissae l for this point as $l_j, j = 1 \dots J$, where J is the total number of such points.

Step 5: Once a new cluster is detected, we have to identify its starting time. Intuitively, l_1 could be considered as the new cluster starting time. However, this may not be the best choice due to noise and the random nature of the channel. Therefore, to select the starting time of the new cluster C_{k+1} , we proceed as follows. For each $j = 1, \dots, J$, we temporarily set $C_{k+1} = l_j$ and do weighted LS fitting of the current exponential cluster between C_k and l_j according to

$$\arg \min_{\alpha_k, \beta_k} \frac{\sum_{i=C_k}^{l_j-1} \mu_i |\ln \hat{P}_i - (\ln \beta_k - (i - C_k)\alpha_k)|^2}{\sum_{i=C_k}^{l_j-1} \mu_i} \quad (19)$$

The value of l_j with the smallest average LS fitting error is chosen as the new cluster starting time, that is $C_{k+1} = l_j$, and the corresponding values of α_k and β_k are used as model parameters for the current cluster.

Step 6: We repeat Steps 4 and 5 until there are no new clusters detected and we let C denote the total number of detected clusters in this way.

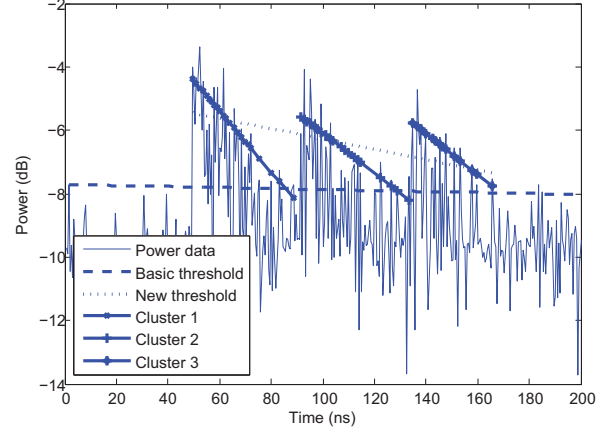


Fig. 2. Illustration of APDP fitting in Log scale.

The fitting in semi-logarithmic scale for several clusters is shown in Fig. 2. The lower straight line is the basic threshold l_{TH_1} . It helps to select the first rough estimate of \hat{D}_r and the corresponding $\hat{P}^{(0)}$. The dotted straight line stands for the new threshold l_{TH_2} that is used to detect the clusters. The 3 clusters are detected and fitted using the 3 short straight lines of varying slopes.

After estimating all the needed parameters C_k, C, β_k and α_k , we can calculate new APDP estimates $\hat{P}_l^{(1)}$ according to (13). After substituting the refined APDP estimate $\hat{P}_l^{(1)}$ back into the log-likelihood function (12), the only unknown parameter left to be estimated is D . The delay D is estimated as the integer value that maximizes the likelihood function. The final likelihood expression $L(D)$ only needs \mathbf{z} , while the background noise spectral density σ_n^2 can be obtained from a *a priori* estimation.

V. SIMULATION RESULTS

In the simulation studies carried out here, the frame duration is set to $T_f = 200\text{ns}$, and each frame is further divided into $N_c = 400$ chips of duration $T_c = 0.5\text{ns}$. The transmitted UWB pulse $w(t)$ is a Gaussian doublet with unit energy, duration T_c and effective bandwidth $B = 4\text{GHz}$. The energy per pulse E_p is given in terms of the SNR parameter E_p/σ_n^2 , where we recall that σ_n^2 is the white noise power spectral density.

The channel impulse responses are based on the IEEE 802.15.4a standard channels, with channel delay spread $\tau_{ds} = 120\text{ns}$ and the number of taps $L = 240$. The maximum delay is $\tau_{max} = T_f - \tau_{ds} = 80\text{ns}$.

On the receiver side, the noisy received signal is passed through a filter matched to a sequence of signed pulses and sampled at the sub-Nyquist rate $1/T_c$. The sub-Nyquist matched filter (correlator) outputs are used to estimate D and P_l as explained in the previous section. The uncertainty region (search range) of the integer delay D is $\{1, \dots, N_c - L\}$. The final TOA estimate, \hat{D} , is selected as the one that maximizes the likelihood function using the value of estimated $\hat{P}_l^{(1)}$.

The accuracy of TOA estimation in this work is evaluated in terms of the root mean square error (RMSE), defined as

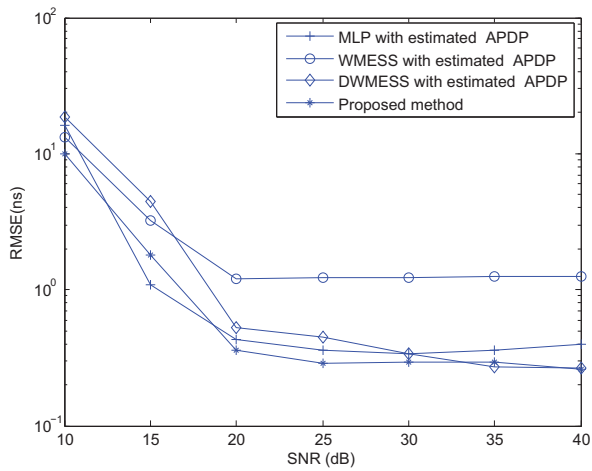


Fig. 3. RMSE of TOA versus SNR for different algorithms.

$\sqrt{E[(\hat{\tau} - \tau_0)^2]}$, where τ_0 denotes the true value of the delay. In the simulations, the expected value is approximated by averaging over 1000 independent trials while the real APDP is fixed. The proposed TOA method is compared with other approaches which also need the prior knowledge of APDP, including WMESS [7], DW-MESS [7] and MLP[6]. All the methods are using the same sub-Nyquist sampling 0.5ns and the estimated APDP to make the comparison fair enough. The window lengths for these methods are set to 120ns, which is the same as the channel delay spread length. The other parameters remain the same as mentioned above.

Fig. 3 shows a comparison of the 4 methods for channel CM3 of IEEE 802.15.4a. While the other 3 methods require *a priori* knowledge of the true APDP, our approach can estimate the APDP in real-time. Applying the estimated APDP to the 3 methods, these estimators still work properly according to the simulation result, which prove that the LS fitting of APDP is applicable in practice. In addition, under the same estimated APDP, the proposed ML estimator shows the best performance among the 4 methods. The proposed method can provide around 0.3ns accuracy.

Fig. 4 shows the performance of the proposed method for different number of frames. According to the figure, the TOA estimation accuracy increases as the number of frames increases. Theoretically, this is due to the averaging operation, which can eliminate the effects of noise

VI. SUMMARY

We proposed and investigated a sub-Nyquist ML-based joint estimator of the TOA and APDP for to IR UWB signals. A parametric model was assumed for the APDP and its parameters were estimated by exploiting a best combination of several LS fitted straight lines. This is in contrast to previous sub-Nyquist methods which assume that *a priori* knowledge of the APDP is available. Through simulations, it was shown that the proposed TOA estimator has a good accuracy and can outperform earlier methods when using the same estimated APDP. Furthermore, since all the digital processing is done at

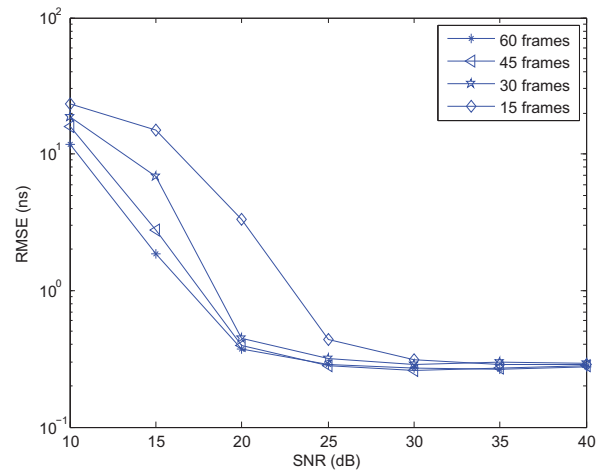


Fig. 4. RMSE of TOA versus SNR for different frame numbers.

the chip rate rather than Nyquist rate, the estimation of the APDP does not add much complexity.

REFERENCES

- [1] M.Z. Win and R.A. Scholtz, "Characterization of ultra-wide bandwidth wireless indoor channels: A communication-theoretic view," *IEEE J. Sel. Areas Commun.*, vol. 20, pp. 1613–1627, Dec. 2002.
- [2] J.Y. Lee and R.A. Scholtz, "Ranging in a dense multipath environment using an UWB radio link," *IEEE J. Sel. Areas Commun.*, vol. 20, pp. 1677–1683, Dec. 2002.
- [3] S. Gezici, Z. Sahinoglu, A.F. Molisch, H. Kobayashi, and H.V. Poor, "Two-step time of arrival estimation for pulse-based ultra-wideband systems," *EURASIP J. on Advances in Signal Processing*, vol. 2008, Article ID 529134, 11 pages, 2008.
- [4] D. Dardari, C.-C. Chong, and M.Z. Win, "Threshold-based time-of-arrival estimators in UWB dense multipath channels," *IEEE Trans. Commun.*, vol. 56, pp. 1366–1378, Aug. 2008.
- [5] J. Youssef, B. Denis, C. Godin, and S. Lesecq, "New TOA estimators within energy-based receivers under realistic UWB channel statistics," in *Proc. IEEE Vehicular Technology Conf. Spring*, Taipei, May 2010, pp. 1–5.
- [6] A. Rabbachin, I. Oppermann, and B. Denis, "ML time-of-arrival estimation based on low complexity UWB energy detection," in *Proc. of IEEE Int. Conf. on Ultra-Wideband*, Waltham, Sept. 2006, pp. 599–604.
- [7] I. Guvenc, S. Gezici, and Z. Sahinoglu, "Ultra-wideband range estimation: Theoretical limits and practical algorithms," in *Proc. of IEEE Int. Conf. on Ultra-Wideband*, Hannover, Sept. 2008, vol. 3, pp. 93–96.
- [8] H. Luecken, C. Steiner, and A. Wittneben, "ML timing estimation for generalized UWB-IR energy detection receivers," in *Proc. of IEEE Int. Conf. on Ultra-Wideband*, Vancouver, Sept. 2009, pp. 829–833.
- [9] A.F. Molisch, K. Balakrishnan, C.C. Chong, S. Emami, A. Fort, J. Karedal, J. Kunisch, H. Schantz, U. Schuster, and K. Siwiak, "IEEE 802.15.4a channel model-final report," *IEEE 802.15 WPAN Low Rate Alternative PHY Task Group 4a (TG4a)*, Nov. 2004.
- [10] Z. Sahinoglu, S. Gezici, and I. Gvenc, *Ultra-wideband Positioning Systems: Theoretical Limits, Ranging Algorithms, and Protocols*, Cambridge University Press, 2008.
- [11] Z. Xu and B.M. Sadler, "Time delay estimation bounds in convolutive random channels," *IEEE J. Sel. Topics Signal Process.*, vol. 1, pp. 418–430, Oct. 2007.
- [12] K. Makaratat, T.W.C. Brown, and S. Stavrou, "Estimation of time of arrival of UWB multipath clusters through a spatial correlation technique," *IET Microw. Antennas Propag.*, vol. 1, pp. 666–673, Jun. 2007.